

Inhibition mechanism of green-synthesized copper-oxide nanoparticles from *Cassia fistula* towards *Fusarium oxysporum* by boosting growth and defense responses in Tomatoes

Hina Ashraf^{(a,b,d,e,f,g)*}, Tehmina Anjum^{(a)*}, Saira Riaz^(b), Irfan S. Ahmad^(c,e),
Joseph Irudayaraj^(d,e,f), Sidra Javed^(a), Uzma Qaiser^(g), Shahzad Naseem^(b)

*For correspondence: hina_ashraf1@hotmail.com; anjum.iags@pu.edu.pk

(a) Institute of Agricultural-Sciences, University of the Punjab, Lahore, Pakistan

(b) Centre of Excellence in Solid-State-Physics, University of the Punjab, Lahore, Pakistan

(c) Department of Agricultural & Biological Engineering, University of Illinois at Urbana-Champaign, IL, USA

(d) Department of Bioengineering, University of Illinois at Urbana-Champaign, IL, USA

(e) Holonyak Micro and Nanotechnology Laboratory, University of Illinois at Urbana-Champaign, IL, USA

(f) Carle Cancer Center/Mills Breast Cancer Institute, Urbana, IL, USA

(g) School of Biological Sciences, University of the Punjab, Lahore, Pakistan.

Supplementary Information

Experiment S1. Characterization of biosynthesized CuO-CFNPs

The absorption spectra of the bio-synthesized CuO-CFNPs solution was monitored by a UV-visible spectrophotometer (Denovix DS-C) in the wave-length ranges from 220-720nm with 1nm resolution. The Fourier transform infrared spectroscopy (FTIR-Thermo Scientific Nicolet 6700) was employed to investigate the functional nature of nanoparticles in a range of 400-4000cm⁻¹ at 4cm⁻¹ resolution in diffuse-reflectance mode by using KBr (potassium bromide) pellets in the ratio of 1:100. To analyze the crystallographic structure of green synthesized copper oxide nanoparticles, X-ray diffraction (XRD) was performed. Philips PANalytical XPert Powder diffractometer with Cu-K α (1.5406 Å) radiation in the range of $2\theta = 20^\circ$ - 80° with an operating voltage of 40 kV at 15 mA was employed to record XRD spectra. The diameter of nanoparticles and zeta potential of CuO-CFNPs were determined by dynamic light scattering (DLS), by using Zetasizer Nano ZS (Malvern Instruments, UK) with a water refractive index of 1.33 at 25 °C to detect size and stability. Morphological and elemental composition was achieved with variable pressure Scanning Electron Microscopy equipped with an EDX instrument (SEM-TESCAN-VegaLMU, 30.0KV) to collect the spectrum. The average size of nanoparticles was analyzed by using Transmission Electron Microscopy (TEM- JEOL 2010F).

Experiment S2. Estimation of Photosynthetic pigments, enzymatic and bioactive compounds

Various bioactive compounds in tomato plants (roots and shoots: at 5th day) and fruit (145th day) were determined after a second foliar spray of different concentrations of nanoparticles. Total chlorophyll and carotenoid content in leaves were appraised by following the protocol of Pocock et al.¹ with minor modifications, while absorbance for Chlorophyll ‘a’ and ‘b’ was acquired at 664 nm and 647 nm, and for carotenoid at 470 nm, according to the formula stated by Wellburn et al.²

$$\text{Chl a} = 12.25 \times \text{Abs}_{664} - 2.55 \times \text{Abs}_{647} \quad (1)$$

$$\text{Chl b} = 20.31 \times \text{Abs}_{647} - 4.91 \times \text{Abs}_{664} \quad (2)$$

$$\text{Total carotenoid} = (1000 \times \text{Abs}_{470} - 1.82 \times \text{Chl a} - 85.02 \times \text{Chl b})/198 \quad (3)$$

Phenolic content in root and shoot was determined by using Folin Ciocalteu reagent at 765 nm as described by Vongsak et al.³ Peroxidase activity (POD) was analysed by guaiacol colorimetric

method at 470 nm as defined by Fu and Hang.⁴ The activity of polyphenol oxidase (PPO) was quantified by the method proposed by Cheema and Sommerhalter,⁵ by using catechol as substrate at 495 nm. The activity of catalase (CAT) was evaluated by decomposition of hydrogen peroxide (H₂O₂) at 240 nm according to Cakmak and Horst.⁶ The activity of Superoxide dismutase (SOD) in the reaction mixture was monitored by inhibition of photochemical reduction of NBT (Nitroblue tetrazolium) at 560 nm, described by Dhindsa et al.⁷ The activity of phenylalanine ammonia lyase (PAL) was determined by using trichloroacetic acid at 290 nm according to Syklowska-Baranek et al.⁸ Protein content in fruit was measured by Bradford method, by taking absorbance at 595 nm with bovine serum albumin used as standard.⁹ Lycopene content in fruits was determined according to Fish et al.¹⁰ by taking absorbance at 503 nm. Vitamin C in fruit was estimated by using 2, 6 dichlorophenol and 2% HCl, as described by Levine et al.¹¹ The quantification of flavonoids in fruit was determined according to the method of Arvouet-Grand et al.¹² by using aluminium trichloride at 415 nm.

Experiment S3. Histochemical Analysis of Tomato Roots and Shoots

Pathogen-challenged and CuO-CFNPs treated tomato plants were harvested after 40 days of treatment. Transverse sections of root and stem were incised by a sharp blade and fixed in FAA (Formalin-aceto-alcohol) for 24 hours. After washing with 70% ethanol, the sections were stained with 10 % Ferric chloride to observe phenolic compounds, by Wiesner's reagent (1% phloroglucinol in 35% HCl) to detect lignification, indicated by fuchsia colour and with Lugol's Iodine / IKI to stain the starch grains, signified by blue to black colouration.¹³⁻¹⁴ Stained sections were mounted carefully on a glass slide and observed under a light microscope (Labomed CSL, Labo America Inc. USA), while, images were captured by a digital camera connected with a microscope.

Supplemental Figures

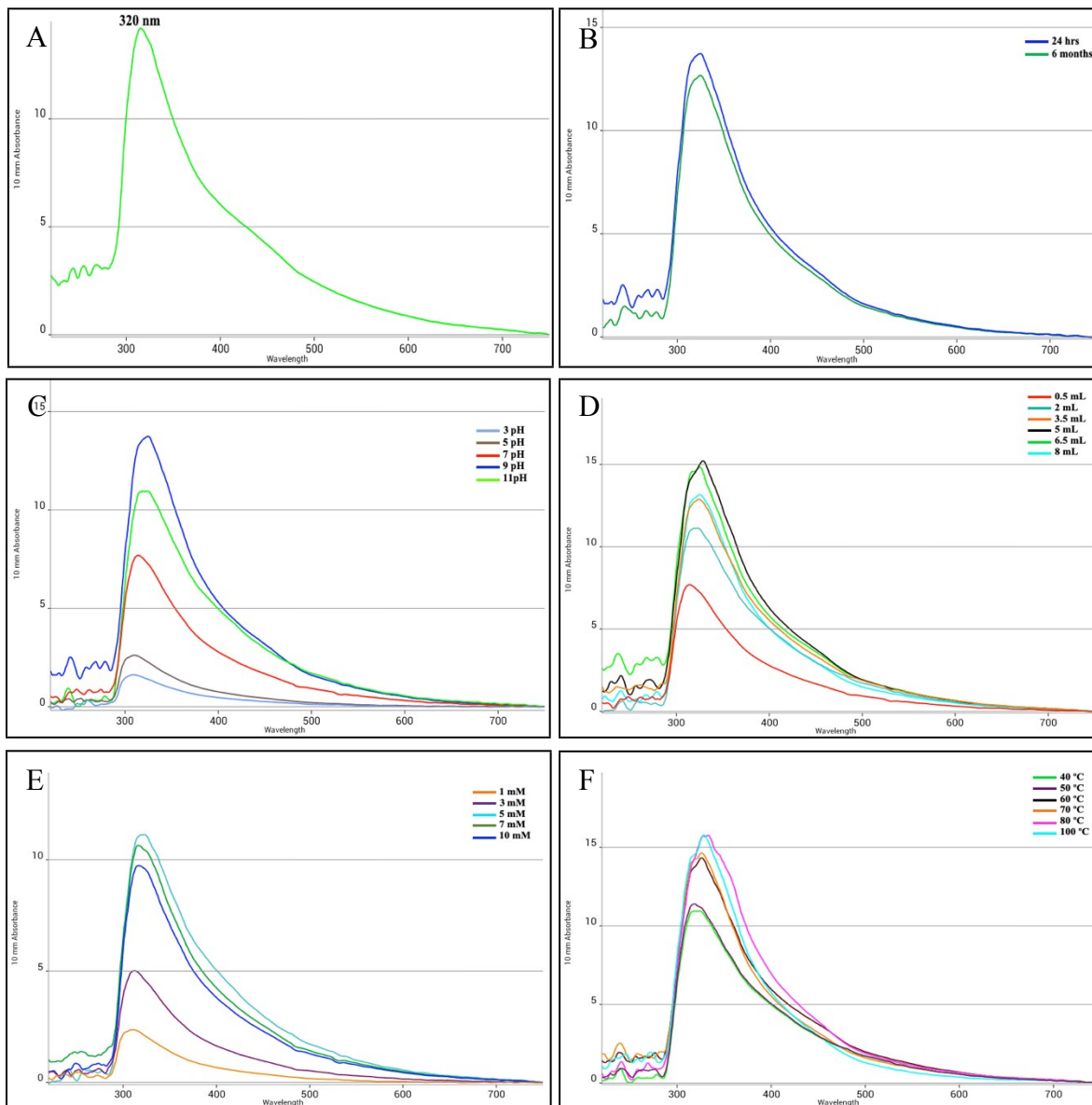


Figure S1: UV-visible absorption spectra of green synthesized CuO-CFNPs at best optimization conditions. UV-visible spectrum under different optimization conditions during synthesis were documented as a function of: (A) UV-visible absorption spectra of CuO-CFNPs. Stability of copper oxide nanoparticles (150mins-6months); (B) pH (9); (C) Amount of CF leaf extract (5mL); (D) copper sulphate concentration (5mM) (E) Temperature (80°C).

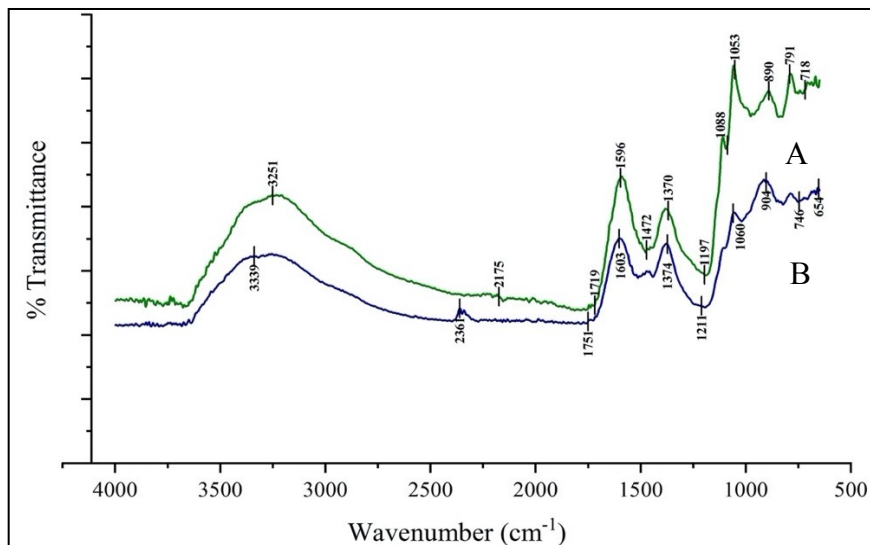


Figure S2. FTIR spectra of synthesized CuO-CFNPs: (A) Spectra of CF-Extract alone. (B) Spectra of CuO-CFNPs.

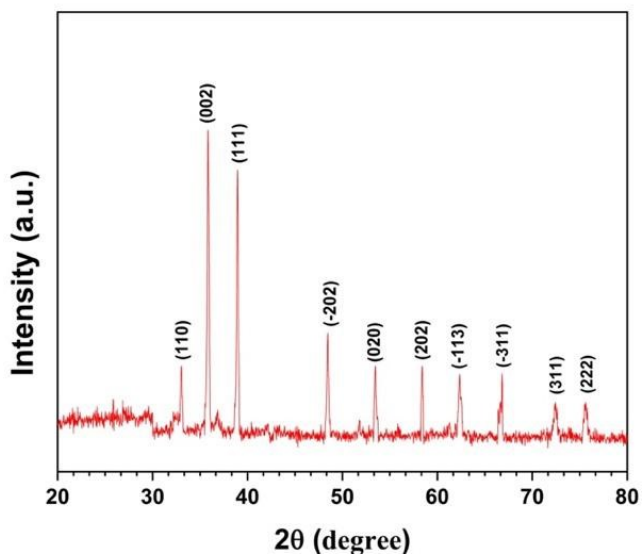


Figure S3. X-ray Diffraction (XRD) Pattern of CuO-CFNPs

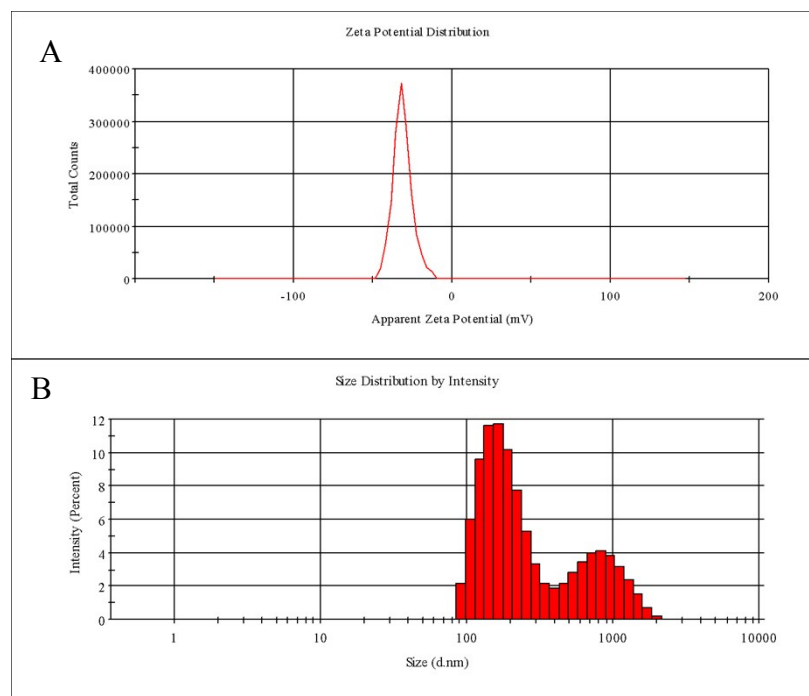


Figure S4. Size distribution intensity and zeta potential distribution of CuO-CFNPs (A&B) as revealed by Dynamic light scattering.

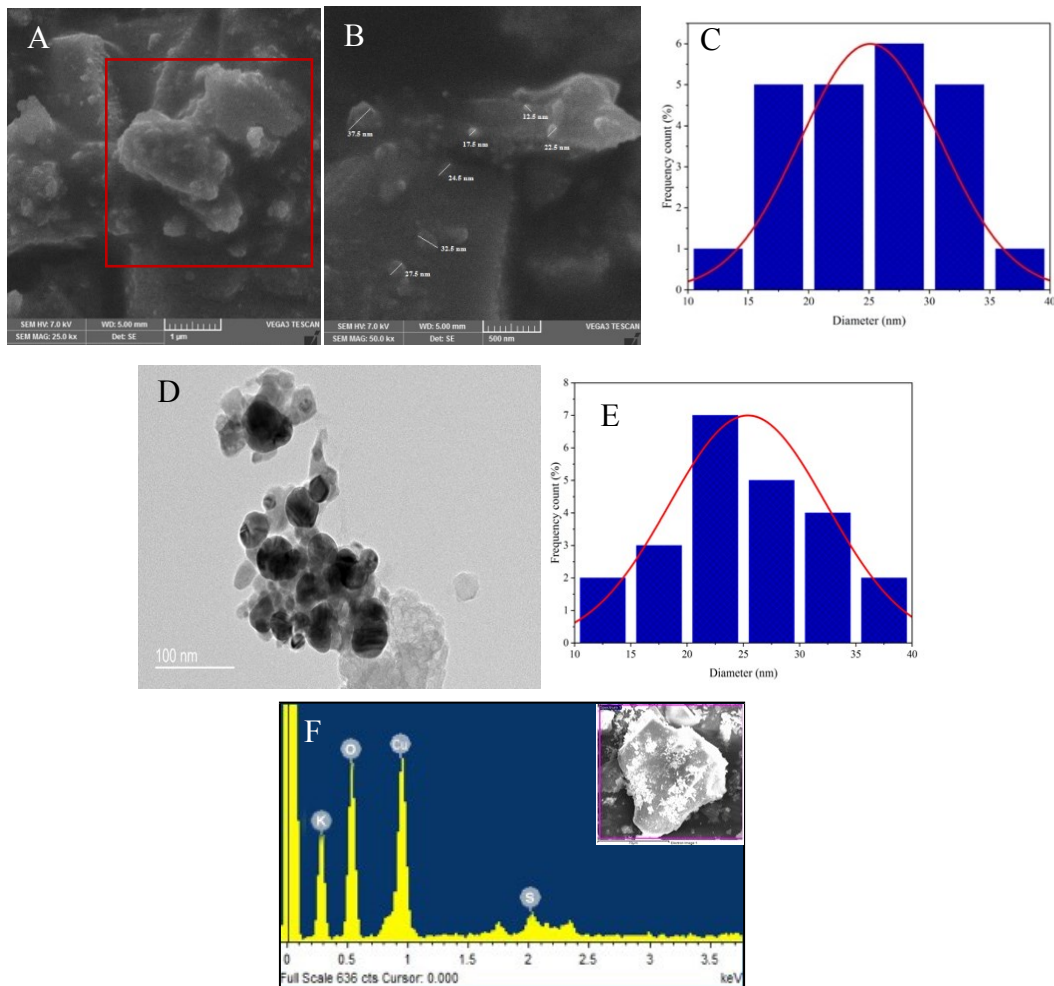


Figure S5. Size analysis of green-synthesized CuO-CF nanoparticles, (A) SEM Image (Scale bar of 1 μ m), (B) Magnified view of SEM (Scale bar of 500 nm), (C) Size distribution analysis of SEM image, (D) TEM image (scale bar indicates 100 nm), (E) Histogram of size distribution of TEM image, (F) Energy Dispersive X-ray (EDX) spectrum of CuO-CFNPs.

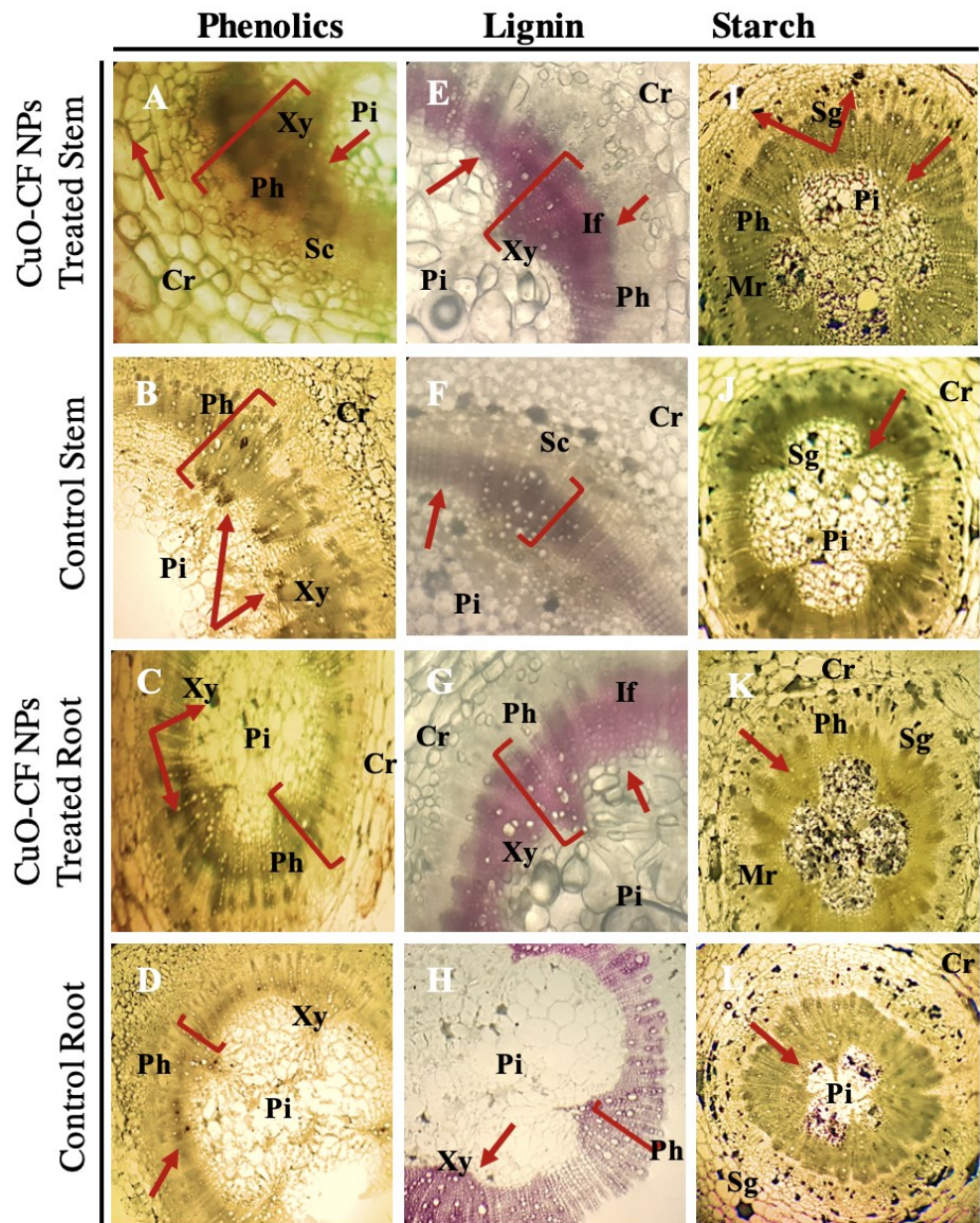


Figure S6. Histochemical analysis of transverse section of tomato root and stem treated with CuO-CFNPs for localization of phenolic (A-D), lignin (E-H) and starch(I-L) at 40x magnification under light-microscope. Cr: Cortex, Pi: Pith, Xy: Xylem, Ph: Phloem, If: Interfascicular-fibers, Mr: Medullary ray, Sg: Starch grains, Sc: Sclerenchyma.

Reference:

1. T. Pockock, M. Król and N.P. Huner, The determination and quantification of photosynthetic pigments by reverse phase high-performance liquid chromatography, thin-layer chromatography, and spectrophotometry, *Methods in Molecular Biology (Clifton, N.J.)*, 2004, **274**, 137–148.
2. A.R. Wellburn, The spectral determination of chlorophylls a and b, as well as total carotenoids, using various solvents with spectrophotometers of different resolution, *Journal of plant physiology*, 1994, **144**, 307–313.
3. B. Vongsak, P. Sithisarn, S. Mangmool, S. Thongpraditchote, Y. Wongkrajang and W. Gritsanapan, Maximizing total phenolics, total flavonoids contents and antioxidant activity of *Moringa oleifera* leaf extract by the appropriate extraction method, *Industrial Crops and Products*, 2013, **44**, 566–571.
4. I. Cakmak, J.W. Horst, Effect of aluminium on lipid peroxidation, superoxide dismutase, catalase, and peroxidase activities in root tips of soybean (*Glycine max*), *Physiologia Plantarum*, 1991, **83**, 463–468.
5. J.M. Fu and B.R. Huang, Involvement of antioxidants and lipid peroxidation in the adaptation of two cool-season grasses to localized drought stress, *Environmental Experimental Botany*, 2001, **45**, 105–114.
6. S. Cheema and M. Sommerhalter, Characterization of polyphenol oxidase activity in Ataulfo mango, *Food Chemistry*, 2015, **171**, 382–387.
7. R.H. Dhindsa, R. Plumb-Dhindsa and T.A. Thorpe, Leaf senescence correlated with increased level of membrane permeability, lipid peroxidation and decreased level of SOD and CAT, *Journal of Experimental Botany*, 1981, **32**, 93–101.
8. K. Sykłowska-Baranek, A. Pietrosiuk, M.R. Naliwajski, A. Kawiak, M. Jeziorek, S. Wyderska, E. ojkowska and I. Chinou, Effect of l-phenylalanine on PAL activity and production of naphthoquinone pigments in suspension cultures of *Arnebia euchroma* (Royle) Johnst, *In Vitro Cellular and developmental Biology. Plant: Journal of the tissue culture association*, 2012, **48**, 555–564.
9. M.M. Bradford, A rapid and sensitive method for the quantitation of protein utilizing the principle of protein-dye binding, *Analytical Biochemistry*, 1976, **72**, 248–254.
10. W.W. Fish, P. Perkins-Veazie and J.K. Collins, A quantitative assay for lycopene that utilizes reduced volumes of organic solvents, *Journal of Food Composition and Analysis*, 2002, **15**, 309–317.
11. M. Levine, A. Katz, S.J. Padayatty, Y. Wang, P. Eck, O. Kwon, S. Chen and J.H. Lee, Vitamin, C. *Encyclopedia of Dietary Supplements*; Marcel Dekker: New York, NY, USA, 2005, 745–755.
12. A. Arvouet-Grand, B. Vennat, A. Pourrat and P. Legret, Standardization of a propolis extract and identification of the main constituents, *Journal de pharmacie de Belgique*, 1994, **49**, 462–468.
13. D.A. Johansen, *Plant microtechnique*, McGraw-Hill, New York, 1940.
14. F.A. Badria and W.S. Aboelmaaty, *Plant Histochemistry: A Versatile and Indispensable Tool in Localization of Gene Expression, Enzymes, Cytokines, Secondary Metabolites and Detection of Plants Infection and Pollution*, *Acta Scientific Pharmaceutical Sciences*, 2019, **3**, 88–100.